JOURNAL OF MATERIALS SCIENCE 23 (1988) 3041–3048

Structure and mechanics of the iris leaf

L. J. GIBSON
Department of Civil Engineering, Massachusetts Institute of Technology, 77 Massachusetts Avenue, Cambridge, Massachusetts 02139, USA

M. F. ASHBY
Cambridge University Engineering Department, Trumpington Street, Cambridge CB2 1PZ, UK

K. E. EASTERLING
Department of Engineering Materials, University of Lueå, Luleå, Sweden S-95187

The structure of the iris leaf resembles that of a sandwich beam with fibre composite faces separated by a low-density foam core. Such structures have a high specific stiffness because the separation of the faces by the lightweight core increases the moment of inertia of the section with little increase in weight. In this paper we examine the structure of the leaf of the bearded iris and show that its flexural stiffness can be explained in terms of the mechanics of sandwich beams.

1. Introduction

For photosynthesis to take place, the surface of a leaf must be exposed to light. Because of this, the leaf must be stiff enough to support its own weight without drooping excessively. Leaves of dicotyledon plants, such as ivy and oak, achieve this stiffness by means of a dendritic network of thick-walled veins. Those of monocotyledons, like the iris and most grasses, derive it largely from a set of parallel ribs running longitudinally along the outer surfaces of the leaf. Fig. 1 shows macrophotos of examples of both arrangements; Fig. 2 shows magnified views of transverse sections of both.

More detailed observation of the microstructure of iris leaves reveals that the stiff ribs, made up of dense sclerenchyma* cells, exist only on the outer skin of the leaf; the bulk of the leaf, inside the outer skin, is made up of thin-walled parenchyma* cells with a lower volume fraction of solids, or relative density (Fig. 2b). The structure is like that of a structural sandwich beam with fibre-reinforced skins separated by a low-density foam core. Such structures have a high specific stiffness as the separation of the stiff faces by the lightweight core increases the moment of inertia of the section with little increase in weight. In this paper we examine the structure of the leaf of the bearded iris and show that its flexural stiffness can be described in terms of the mechanics of sandwich beams. The results should be useful in understanding the mechanical behaviour of other leaves with a similar structure, such as grasses.

2. Structure

A macrophotograph of an iris leaf is shown in Fig. 1d. The width of the leaf is roughly constant for about two-thirds of the length of the leaf; along the final third the width tapers to a point at the tip. The thickness of the leaf varies both along its length and across its width, from a maximum of 6 mm at the centre of the base to about 0.5 mm at the tip and edges. The length of bearded iris leaves is typically between 0.3 and 0.5 m.

Scanning electron micrographs of an iris leaf are shown in Figs 2b and 3. As the sections appear to be undistorted, no special precautions were taken to avoid shrinkage of the specimens during preparation for microscopy. Fig. 2b shows a transverse section; Fig. 3 shows longitudinal sections of the outer ribs and the core of the leaf. These micrographs show that the outer skin of the leaf is made up of dense ribs connected by a single layer of cells of roughly square transverse section; both types of cell run longitudinally along the leaf. Jointly they act like a fibre-reinforced sheet. The cells in the interior of the leaf are different. They are roughly equiaxed in the transverse section (Fig. 2b) and somewhat elongated in the longitudinal section (Fig. 3c). They have extremely thin cell walls and form the low relative density, foam-like "core" of the leaf. A schematic drawing of a transverse section of the leaf, with the central region enlarged to show the leaf dimensions, is shown in Fig. 4. Values for each of the dimensions shown in the figure, measured from several micrographs of specimens taken from two locations along the length of the leaf, are listed in Table I. The results show that with the exception of the depth of the "core" layer, the leaf dimensions remain roughly constant along the length of the leaf. Additional measurements on many iris leaf specimens, made using calipers, show that the depth of the core layer varies from about 6 mm at the base of the leaf to 0.5 mm at the tip.

* Biological terms marked with an asterisk are defined in the Appendix.

0022–2461/88 $03.00 + .12

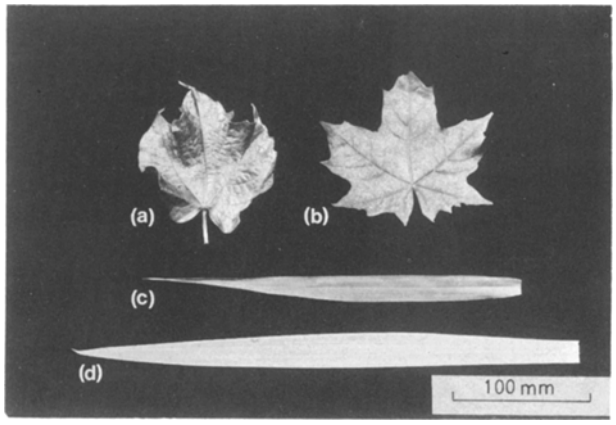

Figure 1 Macro-photographs of (a) ivy, (b) maple, (c) grass and (d) iris leaves. The first two have a network of thick veins to support the leaf; the second two, outer layers of parallel longitudinal ribs, separated by a low-density core.

TABLE I Dimensions of the iris leaf

	Mean (mm)	SD (mm)
At thin end of leaf		
Depth of layer of "face" cells, f	0.03	0.0043
Thickness of square "face" cell wall, t_f	0.0014	–
Length of square "face" cells, l_f	0.04	0.0058
Depth of "core" layer, c	0.5	–
Thickness of "core" cell wall, t_c	0.0014	–
Length of "core" cells, l_c	0.05	0.023
Diameter of rib, d	0.13	0.04
Spacing of rib, s	1.2	0.46
Volume of fraction of solid in rib, V_r	0.8	–
At mid-length of leaf		
Depth of layer of "face" cells, f	0.03	0.0054
Thickness of square "face" cell wall, t_f	0.0014	–
Length of square "face" cells, l_f	0.03	0.0058
Depth of "core" layer, c	3.0	–
Thickness of "core" cell wall, t_c	0.0014	–
Length of "core" cells, l_c	0.07	0.025
Diameter of rib, d	0.19	0.058
Spacing of rib, s	0.92	0.32
Volume of fraction of solid in rib, V_r	0.8	–

3. The stiffness of a sandwich beam

A typical sandwich beam is shown in Fig. 5: it has two thin, stiff faces separated by a lightweight core. The face has a thickness, t, and a Young's modulus, E_f, while the core has a thickness, c, and a Young's modulus, E_c, and a shear modulus, G_c. The width of the beam is b, its length is l. Standard sandwich beam theory (see, for example, Allen [1]) gives the normal stresses in the faces and the core, σ_f and σ_c. If the moment at the section is M, these stresses at a distance z above or below the neutral axis of the beam are

$$\sigma_f = \frac{Mz}{D} E_f \tag{1}$$

and

$$\sigma_c = \frac{Mz}{D} E_c \tag{2}$$

where D, the equivalent flexural rigidity of the sandwich, is

$$D = \frac{E_f b t^3}{6} + \frac{E_f b c (c + t)^2}{2} + \frac{E_c b c^3}{12} \tag{3}$$

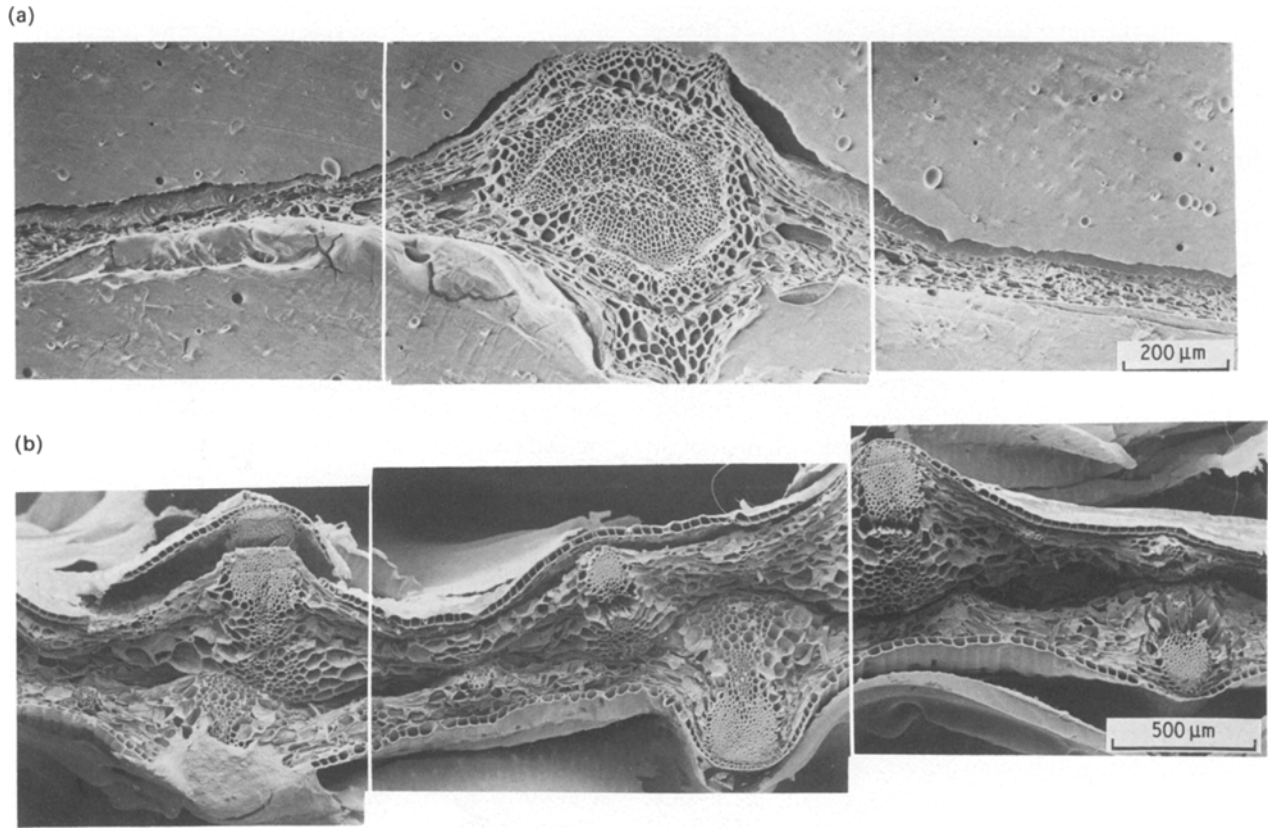

Figure 2 Scanning electron micrographs of transverse sections through (a) an ivy leaf and (b) an iris leaf. In the ivy leaf, the veins run through the centre of the leaf while in the iris, the ribs run along the top and bottom surfaces of the leaf.

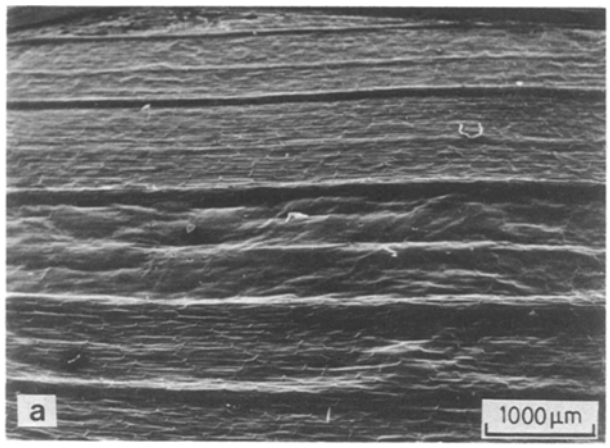

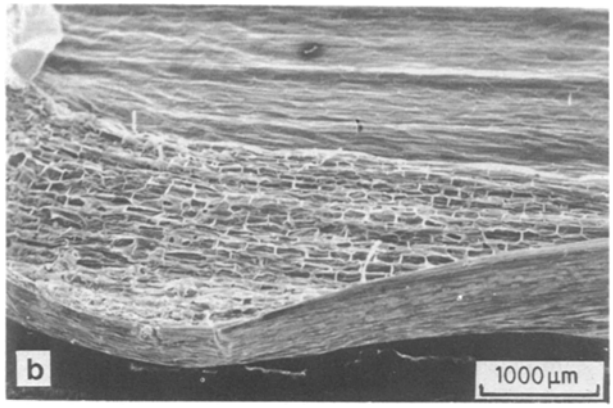

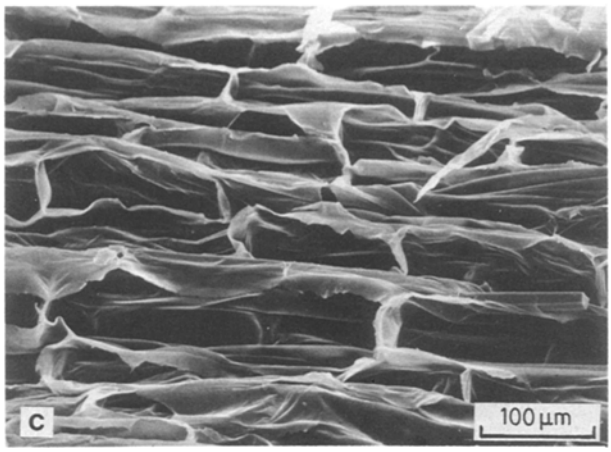

Figure 3 Scanning electron micrographs of longitudinal sections of (a) the outer face, (b) and (c) the inner core of an iris leaf.

or, for sandwich beams with thin faces and a compliant core,

$$D \approx \frac{E_f b t c^2}{2} \tag{4}$$

The shear stress varies parabolically across the faces and core; but, if the faces are thin and the core is compliant relative to the faces, the shear stress distribution becomes almost linear through the faces and constant across the core. At a section where the shear force is V, the shear stress across the core, τ_c, is then given by

$$\tau_c = \frac{V}{bc} \tag{5}$$

The deflection, δ, of a cantilevered sandwich beam under an end load, P, is the sum of the bending deflection, δ_b, and the shear deflection of the core, δ_s

$$\begin{aligned} \delta &= \delta_b + \delta_s \\ &= \frac{Pl^3}{3D} + \frac{Pl}{bcG_c} \end{aligned} \tag{6}$$

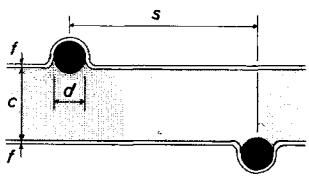

Figure 4 A schematic drawing of a transverse section of an iris leaf showing the variables characterizing its structure.

This gives the stiffness of the sandwich beam in bending, P/δ

$$\frac{P}{\delta} = 1\Big/\left(\frac{l^3}{3D} + \frac{l}{bcG_c}\right) \tag{7}$$

We will make use of this equation in modelling the bending stiffness of the iris leaf. To do so, we require, in addition to the leaf dimensions given in Table I, a value for the Young's modulus of the "face" and for the shear modulus of the "core" of the leaf. These are estimated next.

4. Properties of the "face" and "core" of the iris leaf

To calculate the bending stiffness of the iris leaf in terms of Equation 7, the longitudinal elastic properties of the "face" and "core" must be known. The two Young's moduli, E_f and E_c, can be estimated using a simple rule-of-mixtures if the Young's modulus of the cell wall material, E_s, and the volume fractions of solid in the face and core are known (because the cell walls are aligned in the longitudinal direction). The cell wall modulus, E_s, is estimated below; the volume fractions of solid in the face and core can be found using the cell dimensions listed in Table I. Assuming that the core cells are roughly hexagonal in cross-section and axisymmetric, the longitudinal shear modulus of the core, G_c, is related to the longitudinal Young's modulus, E_c, by [2]

$$G_c = \frac{E_c}{2} \tag{8}$$

4.1. Young's modulus of the cell wall of the iris leaf

The stress–strain curve for plant cell wall material is

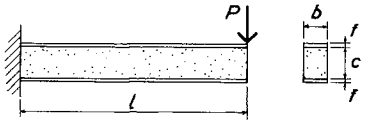

Figure 5 A cantilevered sandwich beam.

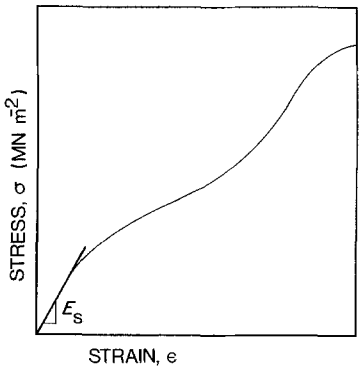

Figure 6 A typical stress–strain curve for the cell wall of a plant (after Preston [4]).

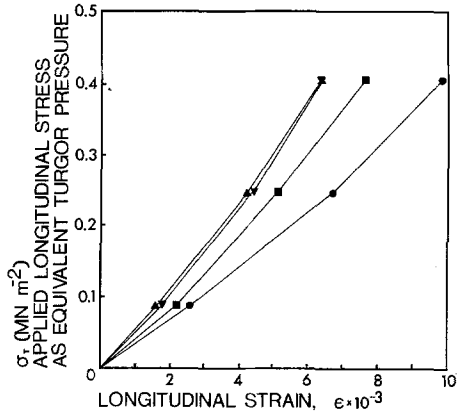

Figure 7 The longitudinal stress plotted against longitudinal strain for a single cell of *Nitella* at various turgor pressures. The stress–strain behaviour is roughly constant at turgor pressures above 0.44 MN m^{-2} (after, [7]). P_t = (●) 0, (■) 0.181, (▼) 0.440, (▲) 0.700 MN m^{-2}.

linear at small strains up to at least 2% [3–5]. Beyond this point it becomes markedly non-linear. A typical curve, taken from Preston [4] is shown in Fig. 6. The Young's modulus of the cell wall material, E_s, is the slope of the initial linear portion of this stress–strain curve.

No data exist for the Young's modulus of the cell wall of the iris leaf. But there are extensive measurements of Young's modulus for the cell walls of other plants and although they are not directly related to the iris, they give an indication of the order of magnitude of the cell wall modulus; they are summarized in Table II. The measured values for the modulus of plant cell walls vary from about 0.12 GN m^{-2} for *Acetabularia crenulata* to 2.2 GN m^{-2} for *Nitella translucens*. Several factors influence the modulus: the most significant are the direction of loading (because the cell wall is made up of cellulose microfibrils helically wound in an amorphous matrix of lignin and hemicelluloses; for a description of modelling the composite nature of cell walls, see Mark [13]) and the moisture content of the cell wall. The rate or the duration of loading has a small effect on the modulus; Sellen [5], for example, measures a decrease in the relaxation modulus of about 20% when the duration of loading is increased by four orders of magnitude.

TABLE II Young's modulus of plant cell walls

Plant Material	Condition (loading time, temperature)	E_s (GN m^{-2})	Reference
Cell wall			
*Penicellus dumetosus**	(0.1 sec, 25° C) wet	0.22	[5]
	(1000 sec, 25° C) wet	0.16	[5]
*Acetabularia crenulata**	(0.1 sec, 20° C) wet	0.14	[3]
	(1000 sec, 20° C) wet	0.12	[3]
*Nitella translucens**	(0.1 sec, 20° C) wet	2.15	[5]
	(1000 sec, 20° C) wet	1.8	[5]
*Nitella opaca**	longitudinal, wet	0.5–1.0	[6]
	tangential, wet	2–4	[6]
Nitella flexilis	wet	0.4–0.7	[7]
Potato tuber	wet	0.5	[8]
Leaf components			
Leaf fibre	dry, θ = 12°	23	[4]
	dry, θ = 22°	12	[4]
Leaf fibre	wet	23	[9]
Leaf bundle	wet	0.84	[9]
Cell wall components			
Cellulose	theory	130	[10]
	theory	27	[10]
Lignin	theory	2	[10]
Fibres with high content of cellulose			
Flax		110	[11]
Ramie		60	[11]
Hemp	wet	35	[12]
	dry	70	[12]
Sisal fibre	dry, θ = 10° room humidity	21	[4]
	θ = 10°	9.8	[4]
	θ = 50°	3	[4]
Cotton hair	dry, θ = 30°	8.5	[4]
	wet, θ = 30°	2.9	[4]
Wood cell wall	θ = 10°	35	[10]
	θ = 35°	10	[10]

*Measurements made on whole cells with cytoplasm removed.
Note that all values of E_s are for loading in the longitudinal direction except where noted by angle, θ.

4.2. Measurement of the cell wall Young's modulus

Measurement of the cell wall modulus directly is difficult because of the small size of the cells. But the modulus can be estimated in an indirect way, by measuring the Young's modulus of the bulk leaf in uniaxial tension and backcalculating the cell wall modulus from the volume fraction of solids in the leaf.

Measurements on the bulk leaf may be affected by the turgor pressure* within the cell: there is some disagreement in the literature on this point. Falk *et al.* [14] measured the longitudinal Young's modulus of specimens of potato tuber at turgor pressures between 0 and 0.66 MN m^{-2}. They found that the modulus increased with turgor pressure throughout this range of pressures. In addition, they found that the measured modulus depended on the cross-sectional area of their specimens; an unexpected result which cast some doubt on the validity of their tests. Kamiya *et al.* [7] have measured the longitudinal stress–strain behaviour of a single cell of *Nicella flexilis* at turgor pressures between 0 and 0.7 Mn m^{-2}. Their results are shown in Fig. 7. They show that the longitudinal stiffness of the cell increases with increasing turgor pressure up to pressures of about 0.4 MN m^{-2}. Above 0.4 MN m^{-2}, the increase in stiffness with turgor pressure is small. We assume that for freshly picked

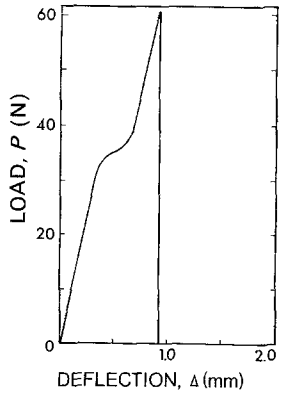

Figure 8 A typical load–deflection curve for the bulk iris leaf loaded in uniaxial tension.

leaves, the turgor pressure is roughly constant at a relatively high level (around $0.6\,MN\,m^{-2}$) so that, following Kamiya *et al.* [7] the longitudinal stiffness of the leaf is unaffected by small changes in pressure.

The water content of the leaf may also affect the measured longitudinal stiffness. Vincent [15] reports that the longitudinal stiffness of two grasses, *Lolium perenne* and *Phleum pratense*, was constant at water contents of between 100 and 400% of the dry weight but rose sharply as the water content was reduced from 100% to 10%. The effect of water content on the stiffness of the bulk iris leaves was measured in the experiments described below.

Rectangular specimens of the bulk iris leaf, roughly 16 mm wide and 48 mm long, were taken from the central portion of the leaf. The width and thickness of each specimen were measured at several points on the leaf to obtain an average value for each. The specimens were then mounted in an Instron testing machine, gripped using standard Instron screw grips and the gauge length was measured. The machine loaded the specimens longitudinally in tension and recorded the load and cross-head deflection on a strip chart recorder. A typical load–deflection curve is shown in Fig. 8. It is linear-elastic up to a deflection of about 0.3 mm, corresponding to a strain of about 0.6%. The load–deflection curve then deviates briefly from linearity before resuming linear behaviour to failure. Tests were done both on fresh leaves and on specimens that had been dried out in an oven to determine the effect of moisture content on the tensile stiffness of the leaf.

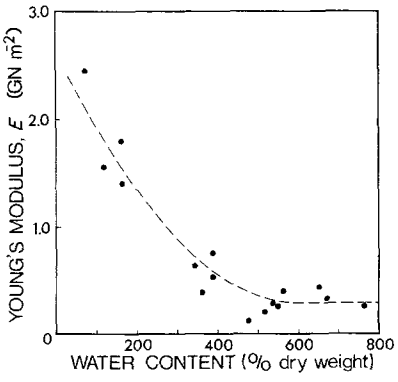

Figure 9 The tensile Young's modulus of the iris leaf as a function of water content.

The water content of each specimen was found by weighing it immediately prior to testing, drying it in an oven for a week after testing it and then reweighing it.

The results are plotted in Fig. 9. They show that above a water content of 500% of the dry weight of the leaf, the tensile stiffness is roughly independent of water content and varies between 0.1 and $0.4\,GN\,m^{-2}$. This large variation in modulus is partly due to the different thickness of leaf specimens tested (and, hence, different volume fraction of stiff ribs in the specimen). The tensile stiffness increases up to $2.2\,GN\,m^{-2}$ as the water content is reduced to 75% of the dry weight.

The modulus of the fresh plant cell wall material can be calculated as follows. A longitudinal tensile stress on the bulk leaf produces longitudinal tension in each component: the ribs, the face cells and the core. The upper bound rule-of-mixtures then gives the measured stiffness of the bulk leaf in terms of the modulus of the solid cell wall material and the volume fraction of solid in each component:

$$E_{meas} = E_s\left[\left(\frac{A_s}{A_0}\right)_{rib} V_{rib} + \left(\frac{A_s}{A_0}\right)_{\substack{face\\cell}} V_{\substack{face\\cell}} + \left(\frac{A_s}{A_0}\right)_{core} V_{core}\right] \quad (9)$$

where $(A_s/A_0)_i$ is the area fraction of solid in the ith component and V_i is the volume fraction of the ith component in the bulk leaf. The area and volume fractions of each component are calculated using the following relationships and the data for the cell dimensions given in Table I; t_l is the thickness of the bulk leaf specimen.

$$(A_s/A_0)_{rib} = 0.8$$

$$V_{rib} = \frac{2(\pi d^2/4)}{t_l s} \quad (10a)$$

$$(A_s/A_0)_{\substack{face\\cell}} = \frac{t_f(f + l_c)}{f l_f}$$

$$V_{\substack{face\\cell}} = \frac{f}{t_l} \quad (10b)$$

$$(A_s/A_0)_{core} = \frac{t_c(l_c + l_c)}{l_c^2}$$

$$V_{core} = 1 - V_{rib} - V_{\substack{face\\cell}} \quad (10c)$$

The thickness and measured tensile stiffnesses of the fresh, bulk leaf specimens are listed in Table III. The area and volume fractions of solid were calculated using Equations 10a to c to give the values of the solid plant cell wall modulus, E_s, in the table: the average value is $4.4\,GN\,m^{-2}$ and the standard deviation is $1.6\,GN\,m^{-2}$. Data in the literature suggest that a typical value for E_s might be about $1\,GN\,m^{-2}$ (Table II); the value calculated here is somewhat higher, but of the same order.

4.3. Calculation of E_f and G_c for the iris leaf

This value can now be used to estimate the longitudinal Young's modulus of the "face" of the iris leaf, E_f,

TABLE III Data for the plant cell wall Young's modulus

Specimen	E_{meas} (GN m^{-2})	t (mm)	E_s (GN m^{-2})
1	0.25	0.61	2.96
2	0.31	0.54	3.55
3	0.31	0.56	3.56
4	0.22	0.68	2.71
5	0.26	0.60	3.16
6	0.11	3.00	3.15
7	0.17	2.50	4.28
8	0.11	3.55	3.43
9	0.41	1.28	7.14
10	0.39	0.76	4.69
11	0.32	1.93	7.11
12	0.26	2.40	6.45

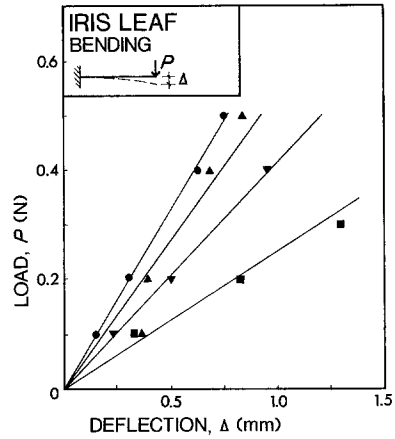

Figure 10 Load–deflection plots for four iris leaf beams. Specimens: (●) 1, (▲) 2, (▼) 3, (■) 4.

and the shear modulus of the "core" of the leaf, G_c. The face modulus is found from the rule-of-mixtures for the ribs and face cells; it is

$$E_f = E_{ribs}\frac{A_{rib}}{A_{face}} + E_{\substack{face\\cell}}\left(1 - \frac{A_{rib}}{A_{face}}\right) \quad (11)$$

where $E_{ribs} = 0.8E_s = 3.52\,GN\,m^{-2}$

$$\frac{A_{rib}}{A_{face}} = \frac{\pi d^2/4}{fs + \pi d^2/4} = 0.39$$

$$E_{face\ cell} = \frac{t_f(f + l_f)}{fl_f}E_s = 0.38\,GN\,m^{-2}$$

$$\frac{A_{\substack{face\\cell}}}{A_{face}} = 1 - \frac{A_{rib}}{A_{face}} = 0.61$$

Substituting the appropriate values from Table II in Equation 11 gives $E_f = 1.61\,GN\,m^{-2}$.

The shear modulus of the core can be calculated from Equation 8 with E_c given by

$$E_c = \frac{t_c(l_c + l_c)}{l_c^2}E_s = 0.21\,GN\,m^{-2} \quad (12)$$

so that the shear modulus, G_c, is $0.105\,GN\,m^{-2}$. As one would expect in a sandwich panel, the stiffness of the face is much greater than that of the core.

5. Measurement of the bending stiffness of the iris leaf

Rectangular specimens of freshly picked iris leaf, 40 mm long and 18 mm wide, were cut for bending stiffness measurements. The thickness of each specimen was measured at both ends and the cross-section of the thickest specimen was sketched. Specimens were clamped between two plates at one end and loaded at the free end 35 mm from the clamped end. Care was taken to ensure that the clamps did not rupture the leaf. Each beam was loaded by hanging a series of five 10 g calibration weights from a chain which was pierced through the leaf. Deflection of the free end of the leaf was measured using a dial gauge with the plunger spring removed to reduce the force required to move it. The load and deflection of each specimen were recorded for loading, unloading and reloading; they are shown for the second loading in Fig. 10. The behaviour is approximately linear elastic; a straight line passing through the origin was drawn through each set of data. The slope of each plot gives the bending stiffness of the beam; the results are listed in Table IV.

6. Discussion: the iris leaf as a sandwich structure

If the iris leaf behaves mechanically like a sandwich

TABLE IV Beam bending results

	Specimen			
	1	2	3	4
Measured beam stiffness, P/δ (N mm^{-1})	0.66	0.54	0.41	0.25
Thickness, t_l (mm)	4.85	3.53	2.71	1.73
Face thickness, f (mm)	0.03	0.03	0.03	0.03
Core thickness, c_1 (mm)	4.63	3.31	2.49	1.51
Core thickness, c_2 (mm)	2.58	2.18	1.78	1.51
Width, b_1 (mm)	6.0	6.0	6.0	6.0
Width, b_2 (mm)	12.0	12.0	12.0	12.0
Flexural rigidity, D (Nm^2)	0.019 1	0.008 96	0.004 62	0.002 1
Bending compliance, $(\delta/P)_b$ (m N^{-1})	0.000 75	0.001 60	0.003 10	0.006 81
Shear compliance, $(\delta/P)_s$ (m N^{-1})	5.7×10^{-6}	7.3×10^{-6}	9.2×10^{-6}	1.2×10^{-5}
Total compliance, (δ/P) (m N^{-1})	0.000 756	0.001 61	0.003 11	0.006 82
Calculated beam stiffness, P/δ (N mm^{-1})	1.32	0.62	0.32	0.15
Calculated P/δ / Measured P/δ	2.00	1.14	0.78	0.60

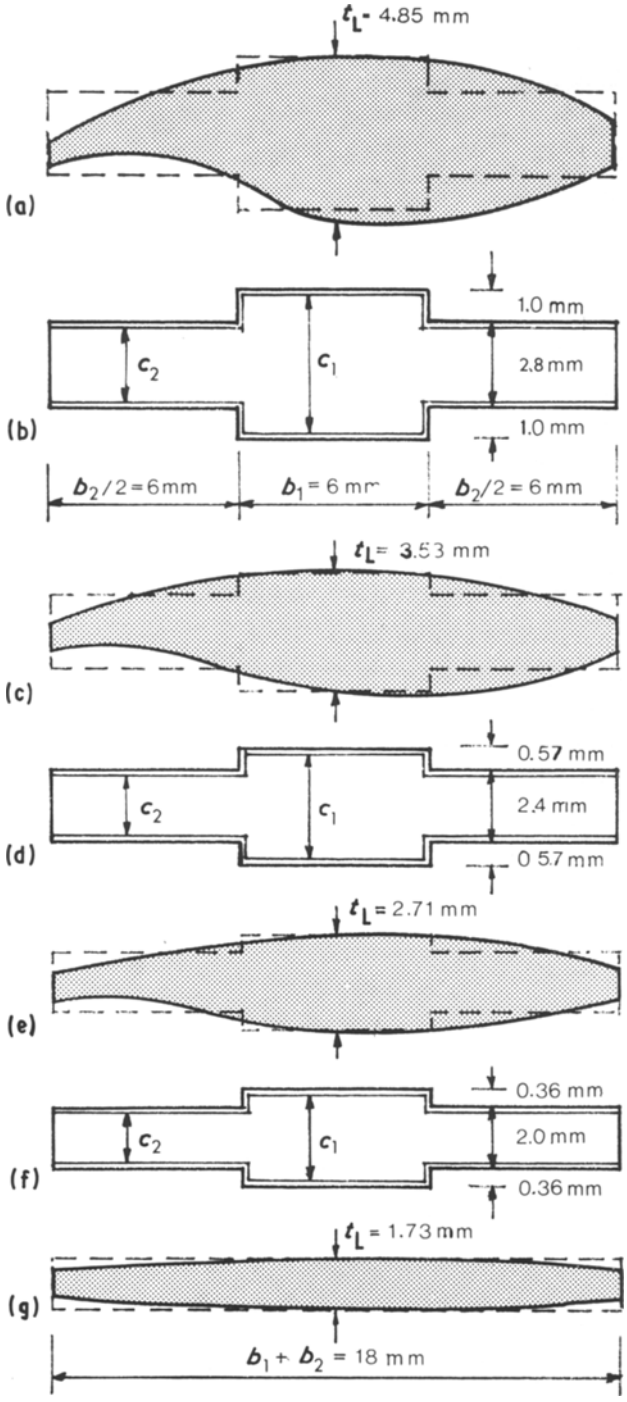

Figure 11 Cross-sections of leaf specimens testing in bending. (a) Sketch of specimen 1, (b) idealization of specimen 1, (c) sketch of specimen 2, (d) idealization of specimen 2, (e) sketch of specimen 3, (f) idealization of specimen 3, (g) sketch of specimen 4.

structure, its bending stiffness can be described by Equation 7. We now calculate this stiffness based on the dimensions of the leaf specimens and on the face and core properties found previously.

The cross-section of the thickest leaf beam bending specimen was sketched before it was tested: it is shown in Fig. 11a. It is irregularly shaped, making computation of its sectional properties difficult. For simplicity, we model it as shown in Fig. 11b. The cross-sections of the other, thinner, specimens can be estimated in a similar way, as is shown in Fig. 11. The dimensions of the model cross-sections are given in the figure and in Table IV.

The water content and turgor pressure of the leaf beam bending specimens were not measured. The specimens were tested on the day they were picked and were kept in water before testing. We assume that their water content is above 500% (as it was for the fresh uniaxial tension test specimens) so that the value of the Young's modulus for the solid cell wall can be taken to be $4.4\,\mathrm{GN\,m^{-2}}$. Similarly, we assume that the turgor pressure in a freshly picked leaf specimen is relatively high (above $0.44\,\mathrm{MN\,m^{-2}}$) so that, following Kamiya *et al.* [7] small changes in it have no effect on the longitudinal stress–strain behaviour of the leaf (Fig. 7). We also assume that small changes in turgor pressure do not affect shearing in the leaf cells as shearing produces no change in the cell volume. As bending produces a combination of longitudinal and shearing stresses in the leaf, we conclude that small changes in turgor pressure do not affect it either.

Using the dimensions of the idealized cross-sections, the equivalent flexural rigidity of the section can be found using Equation 3 by summing the value for each rectangular section. The bending stiffness of each specimen can then be calculated, using Equation 7. The results are indicated in Table 4.

The agreement between the measured bending stiffness of the leaf and that calculated on the basis of sandwich beam theory is as good as could be expected of the approximations made in estimating the moduli of the face and core and in modelling the irregular cross-section of the specimens. The ratio of the calculated to measured bending stiffness is listed in the bottom row of the table; it decreases with decreasing specimen thickness, suggesting an error in the relative thickness of the "face" and "core", or in their moduli. The results support the view that the iris leaf behaves mechanically like a sandwich structure.

7. Conclusions

Micrographs of the iris leaf show that it has a structure not unlike that of a modern ski. The almost fully dense ribs running along the outer faces of the leaf act as stiff fibres much like those in a fibre-reinforced composite. Low-density cells in the core of the leaf separate the faces, increasing the moment of inertia of the leaf with little increase in weight. The leaf, like the ski, thins towards the tip because less stiffness is needed there. Mechanically, too, the iris behaves like a structural sandwich beam. Measurement of the dimensions of the cells and of the Young's modulus of the cell wall material allows the moduli of the "face" and "core" of the leaf to be estimated. From this, the bending stiffness of the leaf can be modelled in terms of the mechanics of structural sandwich beams. Agreement between the measured and calculated bending stiffness of the iris leaf is sufficiently good to conclude that the iris leaf behaves mechanically like a sandwich beam. Many grasses have a structure similar to that of the iris; the sandwich model suggested here may also be of relevance to understanding their mechanical behaviour.

Acknowledgements

The authors would like to thank Professor T.

McMahon for helpful discussions on biomechanics and Mr J. Godlonton for technical assistance.

Appendix. Definitions of some of the biological terms used

Parenchyma [16]: cells of about equal length and breadth, placed side by side, usually soft and succulent, found especially in the softer parts of leaves
Turgor pressure [17]: the excess hydrostatic pressure inside the cell, resulting from the difference between the osmotic pressure of the cell contents and that of the surrounding solution
Sclerenchyma [16]: tissue of higher plants composed of cells with thickened and lignified cell walls.

References

1. H. G. ALLEN, "Analysis and Design of Structural Sandwich Panels" (Pergamon, Oxford, 1969).
2. S. KELSEY, R. A. GELLATLY and B. W. CLARK, *Aircraft Engineering* (October, 1958) 294.
3. P. M. HAUGHTON and D. B. SELLEN, *J. Exp. Bot.* **20** (1969) 516.
4. R. D. PRESTON, "The Physical Biology of Plant Cell Walls" (Chapman and Hall, London, 1974).
5. D. B. SELLEN, in "The Symposia of the Society for Experimental Biology: The Mechanical Properties of Biological Materials", Leeds University, 4–6 September 1979.
6. M. C. PROBINE and R. D. PRESTON, *J. Exp. Bot.* **13** (1962) 111.
7. N. KAMIYA, M. TAZAWA and T. TAKATA, *Protoplasma* **57** (1963) 501.
8. S. B. NILSSON, C. H. HERTZ and S. FALK, *Physiol. Plant.* **11** (1958) 818.
9. J. F. V. VINCENT, *J. Mater. Sci.* **17** (1982) 856.
10. J. BODIG and B. A. JAYNE, "Mechanics of Wood and Wood Composites" (van Nostrand Reinhold, New York, 1982).
11. O. TREITEL, *J. Colloid Sci.* **1** (1946) 327.
12. S. A. WAINWRIGHT, W. D. BIGGS, J. D. CURREY and J. M. GOSLINE, "Mechanical Design in Organisms" (Princeton University Press, Princeton, New Jersey, 1976).
13. R. E. MARK, "Cell Wall Mechanics of Tracheids" (Yale University Press, New Haven, Connecticut, 1967).
14. S. FALK, H. HERTZ and H. I. VIRGIN, *Physiol. Plant.* **11** (1958) 802.
15. J. F. V. VINCENT, *Grass Forage Sci.* **38** (1983) 107.
16. "Oxford Illustrated Dictionary", 2nd Edn (Oxford University Press, Oxford, 1975).
17. S. FALK, H. HERTZ and H. I. VIRGIN, *Physiol. Plant.* **11** (1958) 802.

Received 15 April
and accepted 16 December 1987